Reconstruction of hadronic cascades in large-scale neutrino telescopes

Ralf Auer

Erlangen Centre for Astroparticle Physics, Univ. of Erlangen-Nürnberg, Erwin-Rommel-Str. 1, 91058 Erlangen, Germany

Abstract

A strategy that allows for the reconstruction of direction and energy of hadronic cascades is presented, as well as preliminary results from corresponding simulation studies of the ANTARES twelve-string detector. The analysis techniques are of very generic nature and can thus easily be applied for large-scale neutrino telescopes, such as KM3NeT.

1. Motivation

The primary goal of large-scale neutrino telescopes is the detection of neutrino [1] point sources. In order to achieve the necessary angular resolution, all detectors are optimised for detection and reconstruction of muons that are produced in the charged-current interactions of muon neutrinos with nuclei. Nevertheless, the efficiency of such a detector can be significantly increased by also using other reaction channels: the charged-current electron and τ neutrino reaction and especially all neutral-current reactions.

In reactions without a primary muon, the experimental information comes from the final-state particle cascade (hadronic and possibly electromagnetic), which carries a substantial fraction of the neutrino energy. A reconstruction of energy and direction of such showers would thus allow for measuring
– neutral current events
– charged current ν_e or ν_τ events

and could thus greatly enhance the physics potential of the neutrino telescope. In addition, the shower reconstruction of the hadronic cascades in ν_μ charged current events would allow for a more precise reconstruction of the neutrino energy when the reaction vertex lies within the instrumented detector volume. This will become more and more likely for low-energetic events. Furthermore there is only little atmospheric shower background in the depths those detectors are usually deployed, allowing more reliable diffuse flux detection.

Therefore it is crucial to reconstruct hadronic cascades with the best possible resolution.

2. Reconstruction Techniques

2.1. Basics

When it comes to reconstruction of cascades it is useful to have in mind some major differences of showers as compared to muons: Within some approximation a cascade can be considered to be a point-like light source, at least compared to a muon track. While the muon emits Cherenkov light at a fixed angle (42° in water), the Cherenkov light distri-

---

Email address: `ralf.auer@physik.uni-erlangen.de`;
`Tel: +49 9131 85 27 087; Fax: +49 9131 15 249` (Ralf Auer).
[1] Henceforth no distinction between neutrinos and antineutrinos will be made except where explicitly stated

bution of showers is far more isotropic (as shown in 2.2.1). The photon yield of cascades is much higher than that of muons. As a consequence, the amplitude information from cascade events can be used more reliable than for myon events, especially in case of high background rates. As a consequence of the isotropic light emission and the short lever arm, the angular resolution for cascades cannot compete with that of muons. On the other hand, larger amplitudes and the fact that a shower, unlike a muon, deposits almost all of his energy within the instrumented volume allow for better energy reconstruction.

What will be described here is a very generic approach for the reconstruction of cascades, based on a maximum likelihood method and taking advantage of timing and amplitude information simultaneously. It should be easily adaptable to all kinds of Cherenkov neutrino detectors with only minor modifications.

2.2. *The Modelling*

2.2.1. *Amplitude information*

The observables that have to be reconstructed for the cascade are the energy (E) and the direction (θ, ϕ); an important auxiliary result is the vertex of the interaction (x, y, z).

The probability of a set of parameters in fitting a measured signature in the detector that consists of N detection elements, i.e. photomultipliers, can be expressed by

$$-\ln\left(P^A\right) = -\frac{1}{N} \cdot \sum_{i=1}^{N} \ln\left[p_i^A\left(x, y, z, \theta, \phi, E\right)\right] \quad,$$
(1)

using log-likelihood notation. The superscript A indicates that only the amplitude information is considered in this step. The probability density functions p_i^A are derived from MC simulations. Figure 1 shows the normalised probability distribution of photons as a function of the angle β (between the shower axis and the direction to the photomultiplier) and the amplitude, for water in a depth of 2400 m. Here the five parameters in (1) have been reduced to one parameter, the angle β. What is shown is the projection of the measured amplitude onto the unit sphere around the vertex for an energy range $30\,\text{TeV} \leq E \leq 50\,\text{TeV}$. As can be seen, the photon emission covers the whole angular range from 0° to 180° instead of a sharp peak at 42°; also the amplitude distribution covers several orders of magnitude
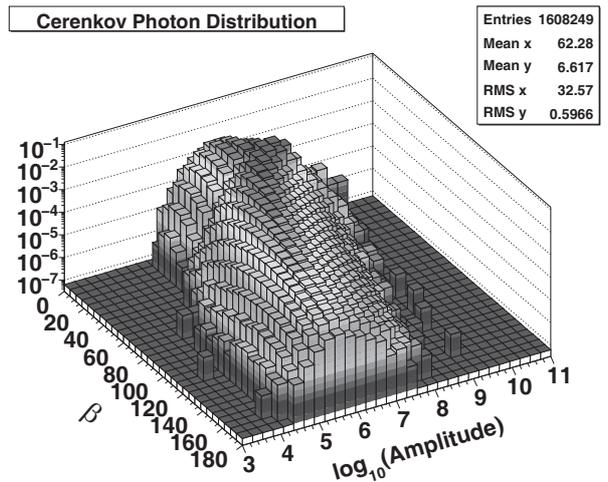

Fig. 1. Probability distribution of the photon flux on the unit sphere around the vertex

already for this tight energy range.

Corresponding MC studies have been carried out for the energy range $100\,\text{GeV} \leq E \leq 10\,\text{PeV}$.

2.2.2. *Timing information*

The timing information can also be taken into account by similar steps.

$$-\ln\left(P^T\right) = -\frac{1}{N} \cdot \sum_{i=1}^{N} \ln\left[p_i^T\left(x, y, z, E, t_0\right)\right] \quad (2)$$

describes the probability that a given set of fit parameters (namely the vertex position, the energy and the time offset, a technical parameter provided by the DAQ system) match the measurement.
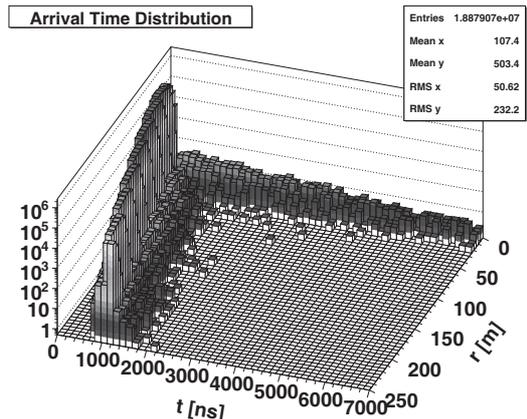

Fig. 2. Arrival time of photons at the photomultiplier including DAQ electronics

Again, the probability distributions are obtained from MC simulations and are shown in Fig. 2 for the
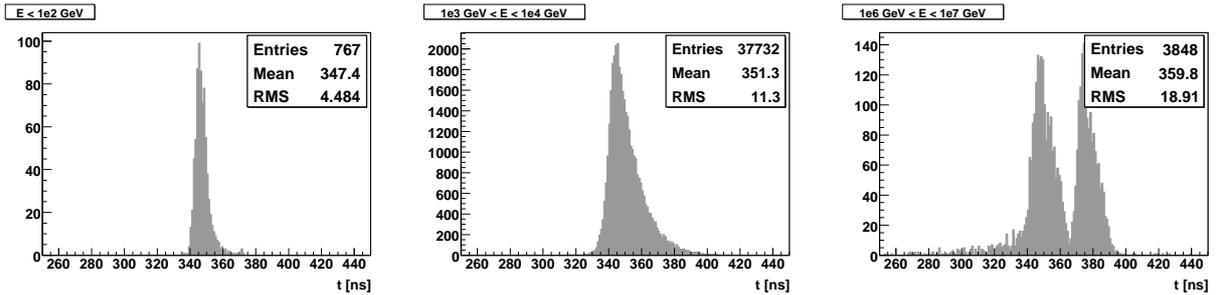
2

E < 1e2 GeV			1e3 GeV < E < 1e4 GeV			1e6 GeV < E < 1e7 GeV		
Entries		767	Entries		37732	Entries		3848
Mean		347.4	Mean		351.3	Mean		359.8
RMS		4.484	RMS		11.3	RMS		18.91

Fig. 3. The effect of the two ADCs per PMT on the photon arrival time distribution for a fixed distance of $r = 70\,\mathrm{m}$ and different energies

whole energy range (10^2 to $10^7\,\mathrm{GeV}$). The spatial variables in (2) are expressed by the Euclidian distance r, while the DAQ parameter t_0 has been set to zero. At this step the full electronic read-out chain of the detector is taken into account. One can clearly see not only the expected linear dependence of the photon arrival time at a photo multiplier on the distance to the photon source, but also DAQ-induced broadening effects (that will be discussed below in more detail) and extremely late photons arriving at photomultipliers close to the vertex. These photons are produced by the decay of low-energy muons from stopped pions, which also explains their short range.

The ANTARES [1] DAQ uses two ADCs per Photomultiplier (PMT), each with an integration window of 25 ns followed by a 250 ns deadtime interval. The dynamic range of the readout is assumed to be 200 single photon electrons (spe).

The influence of the DAQ system can clearly be seen from Fig. 3: For a fixed photomultiplier distance of 70 m the number of detected photons is shown as a function of time for three different energy ranges. For rather small energies (left plot) the photon yield of the shower is quite small and therefore only the first ADC detects photons. At average energies (centered plot) the peak is much broader and also the second ADC detects a small fraction of photons. For very high energies (right plot) both ADCs are saturated, the two peaks are clearly separated. All these effects are taken into account here.

2.3. The Final Model

It is now straightforward to combine timing and amplitude information to find the final expression for the event probability, which depends on seven parameters and one free weighting factor W:

$$-\ln\left(P\right) = -\ln\left(P^A\right) - W \cdot \ln\left(P^T\right) \qquad (3)$$

The task of reconstructing an event can now be reduced to finding the global minimum of this seven-dimensional expression.

2.4. Minimisation

When looking at (3) for specific events in more detail, one can see that $-\ln(P)$ has a very complex structure in the parameter plane with many local minima. In order to find the global minimum, it is crucial to have a very robust minimisation routine that allows not only for traversing local minima, but also performs a wide area scan of the possible phase space.

One routine that accomplishes this task reliably was found to be the implementation of the "Simulated Annealing" algorithm applied by Goffe [3].

3. Preliminary Results

This section shows some preliminary results using the reconstruction method introduced above.

3.1. Reference Detector

The detector used for this study is the ANTARES twelve string detector as deployed in the Mediterranean Sea at roughly 2400 m depth. It consists of 12 *strings* arranged in octagonal geometry with horizontal line spacing of approximately 70 m. Each string is equipped with 25 floors that carry three 10" phototubes each, looking 45° downwards with respect to the horizon. The vertical spacing between the floors is about 14.5 m. The total number of PMTs is 900. The instrumented volume is roughly $200\,\mathrm{m} \times 200\,\mathrm{m} \times 350\,\mathrm{m} \sim 0.01\,\mathrm{km}^3$.
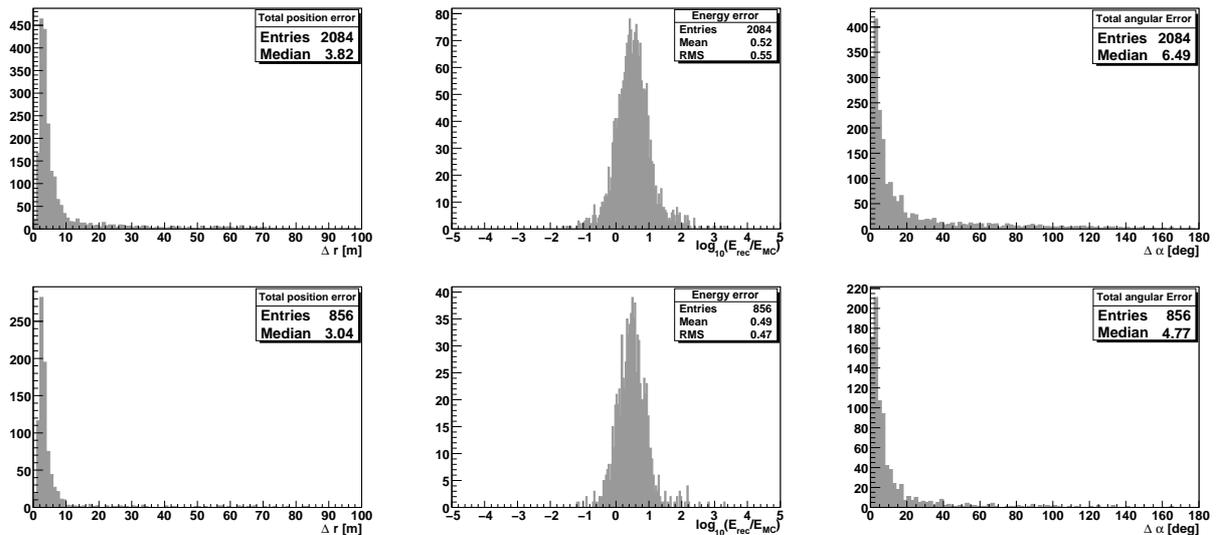
Fig. 4. Preliminary results for position, energy and direction reconstruction without cuts (top row) and with cuts (bottom row)

3.2. *Reference event sample*

The MC event sample was generated using a E^{-1} neutrino spectrum in the energy range $10^2 - 10^7$ GeV. The neutrino direction is distributed isotropically (4π) and the generation volume equals the instrumented detector volume plus roughly one absorption length (55 m) in each direction. A uniformly distributed random background of 120 kHz per PMT has been modulated on all phototubes.

3.3. *Reconstruction constraints*

Due to the rather large amplitudes of showers, small amplitude hits can be neglected in the reconstruction. This allows for a very crude but effective cut to get rid of background hits. Detailed MC studies have shown optimum performance for a cut at three photo electrons. In order to avoid ambiguities in directional reconstruction, a very loose trigger was defined that requests at least 5 hits on 5 PMTs distributed on at least 3 floors and 3 strings.

3.4. *Results*

All events that pass above mentioned trigger are taken into account in the top-line plots of Fig. 4.

The left plot shows the distribution of the total position error, that is the Euclidian distance between reconstructed and MC vertex. The energy resolution is shown in the middle plot, i.e. the logarithm of the ratio of reconstructed to MC shower energy. The right plot shows the total angular resolution, where α describes the angle between reconstructed and MC shower axis. No additional cuts have been applied, thus implying a 100% reconstruction efficiency. Requiring that the reconstructed vertex lies within the instrumented volume allows us to improve the reconstruction significantly as shown in the bottom row distributions in Fig. 4.

4. Conclusion

A strategy for reconstructing cascades in neutrino telescopes was presented. It has also been demonstrated that this reconstruction works well and shows good results for MC studies.

The reconstruction will be applied to ANTARES data and used in KM3NeT [2] studies.

5. Acknowledgements

References

[1] http://antares.in2p3.fr
[2] http://www.km3net.org
[3] W.Goffe: *Simulated Annealing: An Initial Application in Econometrics*, Computer Science in Economics and Management 5(1992),133